ChemCatChem

ChemCatChem
Chemistry Europe
European Chemical Societies Publishing

RESEARCH ARTICLE OPEN ACCESS

Deciphering pH Behavior in Deep Eutectic Solvents: Synergizing Experimental Data and Computational Modeling

Andrea Puglisi[1,2] | Chiara Falcini[3] | Francesco Napoletano[4] | Daniel Alonzo Duránte Salmerón[5] | Marina Cvjetko Bubalo[6] | Gonzalo de Gonzalo[3] | Volker Sieber[7,8,9,10] | André Pick[1,2] | Andrés R. Alcántara[5] | Pablo Domínguez de María[11] | Dinis O. Abranches[12] | João A. P. Coutinho[12] | Selin Kara[4,13]

[1]CASCAT GmbH, Straubing, Germany | [2]Technical University of Munich, Straubing, Germany | [3]Departamento De Química Orgánica, Universidad De Sevilla y Centro De Innovación en Química Avanzada (ORFEO-CIN), Sevilla, Spain | [4]Institute of Technical Chemistry, Leibniz University Hannover, Hannover, Germany | [5]Department of Chemistry in Pharmaceutical Sciences, Complutense University of Madrid (UCM), Madrid, Spain | [6]Faculty of Food Technology and Biotechnology, University of Zagreb, Zagreb, Croatia | [7]Chair of Chemistry of Biogenic Resources, Technical University of Munich, TUM Campus Straubing for Biotechnology and Sustainability, Straubing, Germany | [8]SynBioFoundry@TUM, Technical University of Munich, Straubing, Germany | [9]TUM Catalysis Research Center, Ernst-Otto-Fischer-Straβe1, Garching, Germany | [10]School of Chemistry and Molecular Biosciences, The University of Queensland, St. Lucia, Australia | [11]Sustainable Momentum, SL, Las Palmas de Gran Canaria, Spain | [12]CICECO–Aveiro Institute of Materials, Department of Chemistry, University of Aveiro, Aveiro, Portugal | [13]Biocatalysis and Bioprocessing Group, Department of Biological and Chemical Engineering, Aarhus University, Aarhus, Denmark

Correspondence: Selin Kara (selin.kara@iftc.uni-hannover.de; selin.kara@bce.au.dk)

Received: 3 February 2026 | **Revised:** 12 May 2026 | **Accepted:** 22 May 2026

Keywords: DES | machine learning modeling | pH | pH indicator | UV–vis spectroscopy

ABSTRACT

The expanding application of deep eutectic solvents (DESs) in both upstream and downstream processes has brought increasing attention to the role of pH in these systems. Despite its importance, accurate pH determination in DESs remains a significant challenge, mainly due to the lack of standardized measurement protocols. This has resulted in limited and sometimes contradictory data in literature. In this study, we investigate the acid–base properties of representative DESs using two complementary techniques: pH electrode measurements and UV–vis spectrophotometry with pH-sensitive indicators. The DESs examined include hydrophilic systems based on choline chloride, betaine, and tetrabutylammonium chloride combined with glycerol or ethylene glycol, as well as a hydrophobic lidocaine-oleic acid system. Indicator solutions were titrated with hydrochloric acid, while absorbance and electrode pH values were recorded across each dye's transition range. The resulting absorbance–pH curves were fitted using an inverse Boltzmann model, showing excellent correlation ($R^2 > 0.99$) and enabling reliable interpolation. Additionally, Gaussian process (GP)-based machine learning (ML) confirmed strong agreement between methods within a 95% confidence interval. This integrated approach provides a robust framework for accurate pH assessment in DESs.

1 | Introduction

Deep eutectic solvents (DESs) have garnered considerable attention as a new generation of environmentally friendly solvents with the potential to replace conventional organic solvents and ionic liquids in various (bio)chemical applications [1–7]. DESs are liquid systems typically formed by mixing hydrogen bond acceptors (HBAs), such as methylamines, choline chloride, or

In memory of Prof. Iván Lavandera García, our beloved and dear colleague and friend.

betaine, with hydrogen bond donors (HBDs), such as polyols, organic acids, sugars, or amides. The resulting two-, three-, or multicomponent mixtures often include water as a component added primarily to reduce viscosity. DESs exhibit enthalpy-driven negative deviations from thermodynamic ideality, leading to pronounced melting point depressions compared to their pure components. This phenomenon arises from strong intermolecular (non-covalent) interactions within the mixture, which enable the system to remain liquid even when one or more individual components are solid under the same conditions. Therefore, the identification of a DES requires evaluation of the complete solid–liquid equilibrium (SLE) phase diagram rather than a single mixture ratio, and its composition should not be restricted to whole-number proportions between components [6, 8–10], forming deep eutectic mixtures with a melting point far below than their individual constituents. Although DESs has traditionally been defined by pronounced melting-point depression relative to their individual constituents, recent phase-equilibrium studies have highlighted that kinetic crystallization phenomena and thermodynamic melting behavior are not equivalent. These findings further emphasize that DES formation and classification should be interpreted within a rigorous thermodynamic SLE framework rather than solely through empirical freezing-point depression [11]. DESs are appealing due to their straightforward preparation, low cost, biodegradability, and broad compositional flexibility. These properties enable the rational tuning of characteristics such as viscosity, polarity, thermal stability, and acidity/basicity to meet specific application requirements [1, 8, 12]. This extraordinary tunability, coupled with their generally low volatility and favorable safety profiles, positions DESs as versatile and "designer" solvent platforms capable of supporting applications in (bio)catalysis, electrochemistry, extraction processes, biomass valorization, biosensing, and analytical chemistry while simultaneously aligning with some of the green chemistry principles [13]. Among the wide range of applications, their potential in enzymatic synthesis emerged starting with the pioneering work of Gorke and coworkers [14].

The inherent properties of DESs, such as high viscosity and mass transfer limitations, can be improved by the addition of water as a cosolvent, which facilitates the practical implementation of biocatalytic processes. The addition of water, even at low concentrations, induces structural changes in DESs [15] in terms of (i) viscosity, (ii) conductivity, (iii) density, and (iv) acid/base behavior. Moreover, water can be considered part of the DES, forming a ternary eutectic system [16, 17]. The influence of water on the physicochemical and functional properties of DESs has been extensively investigated employing rheological, spectroscopic, calorimetric, and computational approaches [18–21] to probe how hydration affects these systems. Taken together, results suggest that the addition of water to DESs profoundly influences their nanostructure and macroscopic behavior in a gradient-wise manner, modifying ion pairing [22–28]. At higher water concentrations, a transition is triggered from a DES-dominated structure, often described as a "water-in-DES" regime, where water is confined within the eutectic network, to a "DES-in-water" regime in which the DES components are fully solvated [28–30]. This gradual structural modification underpins the observed changes in transport, solvation, and enzymatic compatibility reported across different DES systems and compositions [22–24, 27, 30].

The transition from a system in which water is segregated within the DES to one in which the components are fully solvated may differ as a function of both the nature of HBA and HBD, and their molar ratio [29]. It is generally accepted that DESs can retain their characteristic supramolecular structure upon the addition of water up to approximately 40–50 wt% (and in some cases up to 57 wt%). Within this range, the strong interactions between components are gradually weakened but remain sufficient to preserve the DES network. At higher water contents, however, the hydrogen-bond network becomes disrupted, and the system progressively behaves like an aqueous solution of the individual components [31]. Therefore, we can conclude that the water content at which this transition occurs depends on the composition of the eutectic mixture [27]. Beyond structural transitions, changes in water content can also influence the acid–base properties of DESs. Strictly speaking, pH is defined as the negative logarithm of the activity of hydrogen [H_3O^+] ions, not just its concentration. Also, pH itself is not equivalent to acidity or alkalinity, which instead describe the buffering capacity of a medium, that is, the resistance to pH changes upon addition of acid or base [32]. The analysis of pH provides insights into the proton activity and the donor/acceptor abilities of DES mixtures, which in turn define the interactions with other compounds. Moreover, the concept of pH in DESs is not directly comparable to the familiar pH scale used in aqueous solutions [33]. While these parameters are relatively straightforward to measure and interpret in aqueous systems, DESs or DES-water mixtures exhibit higher complexity due to factors such as ionic strength, viscosity, and proton activity [34].

Since many catalytic processes are sensitive to pH, understanding how the eutectic composition and hydration level affect the pH of a DES is crucial for designing suitable media. Notable examples of the role of the pH of DESs in various processes can be found in the literature. Zhu et al. systematically compared acidic and alkaline DESs for the pretreatment of grapevine, assessing component removal, lignin structural changes, and antioxidant properties [35]. Strong acidic DES (choline chloride-lactic acid, ChCl-LA) performed comparably to an alkaline DES (potassium carbonate-ethylene glycol, K_2CO_3-LA), removing up to ~60%–81% of hemicellulose and lignin while retaining cellulose. The alkaline DES produced lignin with higher phenolic content, enriched guaiacyl and *para*-hydroxyphenyl units, and greater thermal stability, resulting in enhanced antioxidant activity. This comparative study highlights how DES chemistry can be tailored for both effective biomass fractionation and the generation of lignin streams with added functional value.

Rodríguez Rodríguez et al. showed that sulfonic acid-based DESs, particularly those combined with quaternary salts, ammonium, or phosphonium, represent versatile platforms for metal oxides solubilization [36]. The solubility of a broad set of metal oxides can be enhanced by tuning the HBA:HBD ratio. This tunability highlights the potential of sulfonic acid-based DESs for targeted metal recovery, valorization of low-grade ores, and the use of cheaper alternative HBDs such as methanesulfonic acid. Acidic DESs have also proven effective in fuel purification, particularly in deep desulfurization. Li et al. demonstrated that the accurate selection of the HBA increased the extraction efficiencies, reaching 82.8% in a single cycle and 99.5% after five cycles, thereby lowering the sulfur content in fuels to below 8.5 ppm [37]. Yin

et al. reported a positive correlation between DES acidity and desulfurization performance, achieving efficiencies of 97.2% and 95.9% using choline chloride- or tetrabutylammonium chloride-based *p*-toluenesulfonic acid DESs, respectively, highlighting acidity tuning as a powerful strategy for fuel purification [38].

Monitoring the pH of a DES-based system in biocatalysis is also critical, as many enzymes are susceptible to changes in their acid–base environment. Liu and Shi [39] examined lipase-catalyzed esterifications in several hydrophilic non-acidic, acidic, and hydrophobic DESs, observing that a pH shift of ~3 units could alter enzyme activity by more than 30%, with significant inhibition at acidic conditions.

Baby et al. systematically investigated NADH-dependent formate dehydrogenase activity in DES/buffer/water mixtures, demonstrating that both pH and water activity significantly influence enzyme performance and stability, with optimal activity achieved through appropriate buffer addition [40]. Xu et al. reported that the optimal pH for alcohol dehydrogenase-catalyzed bioreduction in a choline chloride:ethylene glycol DES shifted to pH 5.0, emphasizing that the preferred pH range depends strongly on the enzyme, substrate, and solvent composition [41]. Similarly, Zhang et al. examined horse liver alcohol dehydrogenase in different DESs and found that maintaining a favorable pH environment, together with suitable water content, is essential for preserving enzyme activity and stability [42].

Despite the above-discussed examples, and although the high relevance of pH in DESs is evident, studies reporting experimental values of pHs of DESs are scarce compared to the systematic studies reporting other physicochemical parameters of DESs, such as viscosity or conductivity. Furthermore, the influence of DES components, their molar ratio, and the presence of water on their pH remains to be understood.

Hayyan et al. studied sugar-based DESs, measuring the pH at different HBA-HBD molar ratios and temperature [43, 44]. The results showed that the pH decreased with increasing temperature (from 25°C to 85°C), also depending on the ChCl:fructose molar ratio. The 1:1 and 1:2 ratios showed substantial pH decreases, whereas the 1:1.5 and 1:2.5 ratios exhibited only slight reductions. Similar results were obtained for ChCl:glucose at different molar ratios, where the pH value of the neat DES was almost neutral. Conversely, the system displayed low sensitivity to temperature variations. Additionally, Skulcova et al. reported that the pH values of ChCl-based systems decreased with increasing temperatures (a drop of 0.69 units from 20°C to 60°C) [45]. Mitar et al. showed that organic acid-based DESs exerted higher acidity compared to those mixtures using polyalcohols [46]. The water content affected the pH of DESs, and thus, for systems with extremely low pH, increasing the water content resulted in higher pH values. In contrast, within the higher pH range, the pH decreased with increasing water content.

In the literature, several strategies have been employed to measure pH in DESs, including potentiometric [12], as well as methods aimed at determining apparent acid dissociation constants through potentiometric titration, UV–vis spectroscopy [12, 34], and NMR [47]. Additionally, computational approaches (mainly based on COSMO-RS) [1, 8] have been reported to predict pH values. Each approach provides valuable insights but also presents some limitations when applied to these complex mixtures. Among these strategies, it is worth highlighting the work of Abbot and coworkers in 2017 [34], where the pH behavior and proton activity in DESs were investigated using standard pH indicator solutes, such as bromophenol blue. The DESs were titrated with triflic acid, allowing for a deeper understanding of the pH dynamics. Remarkably, the technique yielded valuable insights into the behavior of the glass electrode in DESs. Although the water content decrease led to a deviation from ideal Nernstian behavior, suggesting that the potential did not vary proportionally with the logarithm of ion concentration, the response was linear and correlated with the pH indicator method.

While reported studies provide useful benchmarks, the variability and, in some cases, discrepancy among published pH values underscore the need for a standardized and readily implementable method. In this work, we present a synergistic, comparative approach that combines direct pH electrode measurements with UV–vis spectroscopy using pH-sensitive indicator molecules to determine the pH of a representative set of DESs. Briefly, the inverse Boltzmann equation was employed to fit experimentally obtained pH values from the calibration curve of each dye with the corresponding absorbance measured by a UV–vis spectrophotometer. By training and fitting on both data sources simultaneously, a stochastic machine learning (ML) framework based on Gaussian process (GP) models was employed to reconcile discrepancies between the datasets and to quantify uncertainty by assigning confidence intervals to the pH measurements reported in this work. Systems studied include hydrophilic systems based on choline chloride (ChCl), betaine (Bet), and tetrabutylammonium chloride (TBAC) combined with glycerol (Gly) or ethylene glycol (EG) as HBDs, and one hydrophobic system, lidocaine-oleic acid (Lid-OA), which has been reported in the literature to display distinct behavior [48, 49]. These DESs have been chosen due to their wide application in both biocatalysis and chemical processes. Using the dual experimental method, together with the ML modeling, we investigated how water addition affects the acid–base environment of DESs and examined the impact of added buffers on the apparent pH.

2 | Results and Discussion

2.1 | Experimental Analysis of the pH of DESs—Buffer Mixture

The pH values of DESs were determined experimentally using two methods: (i) an electrochemical sensor and (ii) molecular dyes. In the first method, a conventional glass pH electrode was used to measure the proton activity in the DESs. The electrode detects the potential difference generated by the selective interaction of hydrogen ions with the glass membrane, which correlates with the pH of the medium. In the second method, pH-sensitive indicator dyes were used to assess proton activity in the DESs. The protonation or deprotonation of the indicators was monitored by UV–vis spectroscopy. For the selected dyes, any changes in absorption within the 350–700 nm range reflect shifts in the local proton environment (for further details, see the Supporting Information).

TABLE 1 | Structure of DES components.

HBA		HBD		DES			
Name	**Structure**	**Name**	**Structure**	**DES abbreviation**	**Molar ratio**	**T_m (°C)**	**References**
ChCl	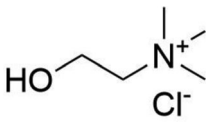	Gly	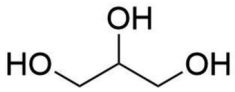	ChCl-Gly	1:2	−36.15	[50]
		EG	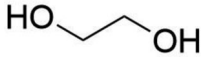	ChCl-EG	1:2	−28.00	[11]
Bet	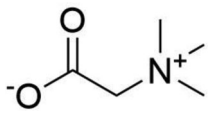	Gly	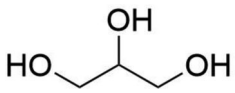	Bet-Gly	1:2	n/a	—
		EG	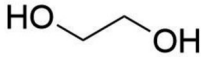	Bet-EG	1:3	n/a	—
TBAC	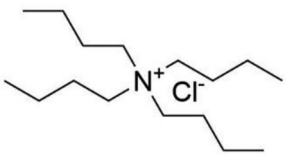	Gly	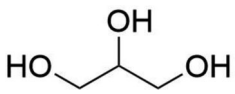	TBAC-Gly	1:3	−41.64	[51]
		EG	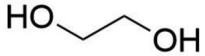	TBAC-EG	1:3	−30.88	[51]
Lid	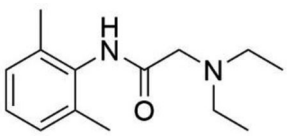	OA	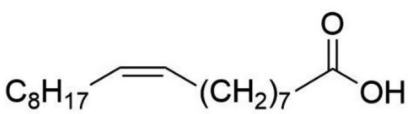	Lid-OA	1:1	n/a	—

Note: n/a: not available in literature.

Abbreviations: ChCl—choline chloride, Gly—glycerol, EG—ethylene glycol, Bet—betaine, TBAC—tetrabutylammonium chloride, Lid—lidocaine, OA—oleic acid.

In total, four case studies were considered, using different HBAs, choline chloride (ChCl), betaine (Bet), and tetrabutylammonium chloride (TBAC) in combination with two HBDs, namely, glycerol (Gly) and ethylene glycol (EG). In addition to these hydrophilic DESs, an exemplary hydrophobic lidocaine-based DES was also applied (Table 1). For each HBA-HBD (mol:mol) combination, the pH of the pure DES, with increasing mass fractions of ultrapure water (pH of 6.31), was measured. Additionally, the pH of DESs with 20 wt% buffer (sodium acetate (NaOAc), pH 4.68; potassium phosphate (KPi), pH 5.92; and 2-amino-2-(hydroxymethyl) propane-1,3-diol (tris), pH 9.00, each of them having two different final concentrations: 10 and 100 mM) were assessed to determine whether the pH of the DESs is influenced by the buffer type and/or ionic strength. The choice of dye for each DES was guided by the pH values previously measured using a pH electrode (all the measurements were performed at 25°C), as well as by the pKa range of the selected dye.

2.2 | Case Study 1—Choline Chloride–Based DES

The ChCl-based DESs were studied in combination with Gly and EG as HBDs. The analyses were conducted on the two neat DESs (ChCl-Gly and ChCl-EG; both at 1:2 mol/mol) with the addition of ultrapure water (0–80 wt%), using either (i) the pH electrode or (ii) the bromothymol blue pH indicator (adapted to the pH range of those DESs).

As shown in Figure 1a, the addition of water to ChCl-Gly (1:2) results in a slight increase in the system's acidity, in agreement with the literature, which reports that the pH of the DES system decreases with increasing water content. For neat ChCl-Gly, a pH of 6.54 and 6.70 was measured with the pH indicator and electrode, respectively; this value was found to be in agreement with Yee Tong Tan et al. (2018) [52]. When prepared with 30–80 wt% water, the pH values varied within a range from 6.03 to 5.32 and 6.49 to 5.83 using the pH indicator and electrode (Figure 1a). Conversely, a more acidic pH, ranging between 3.71 and 3.06, with the same water content, was reported by Panić and coworkers [8]. For ChCl-EG in the same conditions, pH values of 6.81 to 6.38 and 6.81 to 6.34 with pH indicators and electrode, respectively, were obtained (Figure 1b). Nevertheless, a rather large discrepancy was observed when compared with data reported by Panić et al. [8] at high-water-content conditions (50 and 80 wt% water), as these authors observed pH values of 4.58 and 4.41 (Table 2). Both methods for pH measurements yielded similar results, with a slight acidification of the ChCl-based DESs as the water content increased, possibly due to the dissociation of water, which generates more detected protons and changes the system from binary to ternary [18]. Finally, GP modeling yields a

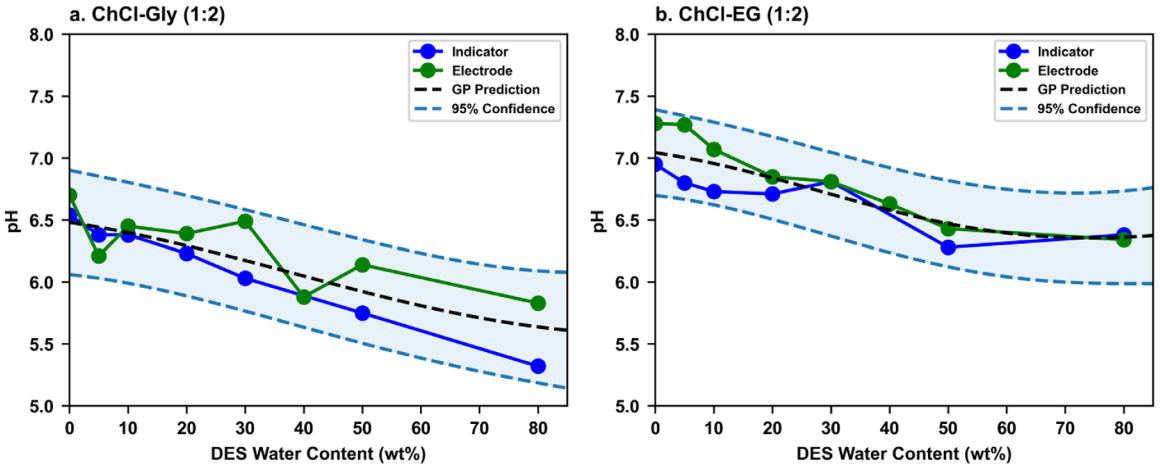

FIGURE 1 | Measured values for ChCl-Gly (1:2) (a) and ChCl-EG (1:2) (b) with different water fractions, using an electrochemical pH detector (green line) or UV-vis spectrophotometry with the addition of bromothymol blue (absorbance at 615 nm, blue line). All measurements were conducted in triplicate. Predictions (black dashed line) with 95% confidence (blue dashed lines) intervals from GP models simultaneously fit to both data sources are also included.

narrow 95% confidence interval in regions where all experimental data are incorporated, thereby validating and corroborating both pH measurement approaches. Note that GP models do not predict scalar values, as described in Supporting Information. Instead, they predict Gaussian probability distributions for the output, with the mean of that distribution being considered the GP-predicted scalar value for the output, and the standard deviation of that distribution being considered a measure of the inherent uncertainty of the GP about that prediction. Importantly, the width of this 95% confidence interval is, for all cases, narrower than 1 pH unit.

No difference was observed in the role of protonation provided by the water, regardless of the change in the HBD in the system, and no studies to date have been found in the literature. Encouraged by these initial results, the effect of adding a buffer was studied, also comparing the two pH measurement methods mentioned above. The buffer solutions were added to the initial samples to reach a 20 wt% aqueous content. In total, three different buffers (NaOAc, KPi, and tris base) at two ionic strength levels (10 and 100 mM) were screened to evaluate the pH effect of their addition to the final DES formulations (Figure 2).

For the ChCl-Gly (Figure 2a), the addition of NaOAc buffer (10 or 100 mM) led to a 2-unit pH decrease for the dye-based measurement, from 6.23 to 4.24, while just 1 unit pH decrease, from 6.41 to 5.46, was observed when the measurement was carried out with the pH electrode. In the case of ChCl-EG (Figure 2b), the observed decrease in pH values upon addition of the NaOAc (10 or 100 mM) buffer was similar in both measurement methods. Here, a decrease of 1 pH unit, from 6.71 to 5.55 with the dye and 6.90 to 5.92 with the pH electrode, was detected. Overall, similar results were obtained when using two different ionic strengths across the tested buffers, regardless of the experimental method employed. The discrepancy in pH measured with the two methods when NaOAC is used in ChCl-Gly suggests some particular interactions among the DES components and the buffer with the pH method. These interactions have never been assessed and would require further in-depth work to understand the rationale behind.

2.3 | Case Study 2—Betaine-Based DES

Taking betaine as HBA, Gly, and EG were evaluated as HBDs. However, unlike the previous analysis, for betaine-based DES, Gly was used at a 1:2 ratio, and EG was used at a 1:3 ratio. The reason for this choice is due to the low stability of the Bet-EG 1:2 ratio, which undergoes crystallization after preparation during the cooling step. Moreover, the 1:3 molar ratio has already been reported and thoroughly characterized in the literature [9, 53, 54]. Once again, bromothymol blue was used as a pH indicator molecule for this case study.

The analysis of betaine-based DESs revealed an alkaline pH, albeit upon addition of water (up to 80 wt%), a significant change in pH, for example, from 8.71 to 6.90, was observed (Figure 3a), indicating a more substantial influence of betaine on the final pH for the DESs formulation compared to ChCl. The progressive addition of water exhibits a neutralizing effect, as also observed by Panić et al. [8] (Table 2). Results from the pH-meter analysis and the UV–vis for the pure DES and DES-water mixtures are shown in Figure 3.

As reported in Figure 3a, neat Bet-Gly (1:2) revealed a pH of 8.71 and 8.07 from the electrochemical detection and spectrophotometric, respectively. In this case, in contrast to the systems presented in Figure 2, the GP-predicted confidence interval exceeds 1 pH unit, most likely because of the systematic offset observed between the indicator and electrode datasets. Neat Bet-EG (1:3) exhibited pH values of 8.84 and 7.76, as determined by the two methods (Figure 3b). Despite the different values, both data points are contained within the narrow 95% confidence interval assigned by the GP modeling. Finally, the two systems did not display significant differences related to the different HBDs, possibly due to the presence of a total of six hydroxyl groups

TABLE 2 | Experimentally measured pH values and comparison with literature.

DES (HBA-HBD)	HBA-HBD, mol:mol	H_2O (wt%)	pH (indicator) ± std	pH (electrode) ± std	pH (literature)	References
ChCl-Gly	1:2	0	6.54 ± 0.03	6.70 ± 0.10	6.69	[52]
					3.54	[55]
					4.43	[56]
					6.97	[57]
					5.00	[58]
					2.46	[59]
					6.95	[60]
					7.54	[61]
					4.72	[62]
		10	6.38 ± 0.02	6.45 ± 0.23	4.47	[45]
					6.95	[63]
					3.85	[55]
		30	6.03 ± 0.02	6.49 ± 0.14	3.71	[8]
					6.03	[63]
					3.75	[56]
					3.30	[64]
		50	5.75 ± 0.03	6.14 ± 0.15	2.67 ± 0.1	[8]
					5.68	[63]
					3.75	[56]
					3.50	[64]
		80	5.32 ± 0.09	5.83 ± 0.13	3.06	[8]
					4.89	[63]
					3.90	[64]
ChCl-EG	1:2	0	6.95 ± 0.00	7.28 ± 0.06	4.51	[55]
					4.49	[56]
					5.93	[57]
					7.02	[60]
					3.42	[65]
		10	6.73 ± 0.01	7.07 ± 0.12	6.19	[8]
		30	6.81 ± 0.01	6.81 ± 0.01	6.60	[8]
					4.04	[56]
					7.10	[64]
		50	6.28 ± 0.01	6.43 ± 0.02	4.58	[8]
					3.89	[56]
					6.00	[64]
		80	6.38 ± 0.00	6.34 ± 0.01	4.41	[8]
					5.20	[64]

(Continues)

(two times $(HOCH_2)_2CHOH$ and three times $HOCH_2CH_2OH$) equivalents in both DES formulations.

The weak alkaline nature of betaine-based DESs has already been reported in the literature [9]. This behavior (Figure 3) can be attributed to the zwitterionic form of betaine, which exhibits a quaternary ammonium group and a carboxylate group ($pK_a = 1.8$). While the former is not viable for proton transfer, the latter can act as a proton acceptor, acting as a weak base. The neutralizing effect of water addition was determined by Panić et al. [8], where

TABLE 2 | (Continued)

DES (HBA-HBD)	HBA-HBD, mol:mol	H_2O (wt%)	pH (indicator) ± std	pH (electrode) ± std	pH (literature)	References
Bet-Gly	1:2	0	8.07 ± 0.24	8.71 ± 0.18	7.56	[9]
					5.38	[66]
					5.50	[67]
		10	7.74 ± 0.10	8.54 ± 0.03	4.73	[63]
		30	7.08 ± 0.04	8.06 ± 0.06	6.77	[8]
					4.26	[63]
		50	6.72 ± 0.01	7.52 ± 0.03	6.37	[8]
					3.87	[63]
		80	6.22 ± 0.01	6.89 ± 0.13	3.75	[63]
Bet-EG	1:3	30	7.17 ± 0.00	7.44 ± 0.03	6. 86 (molar ratio 1:2)	[8]
TBAC-Gly	1:3	0	2.58 ± 0.15	1.88 ± 0.24	6.51–6.11	[51]
TBAC-EG	1:3	0	3.44 ± 0.01	4.43 ± 0.05	9.20–7.72	[51]

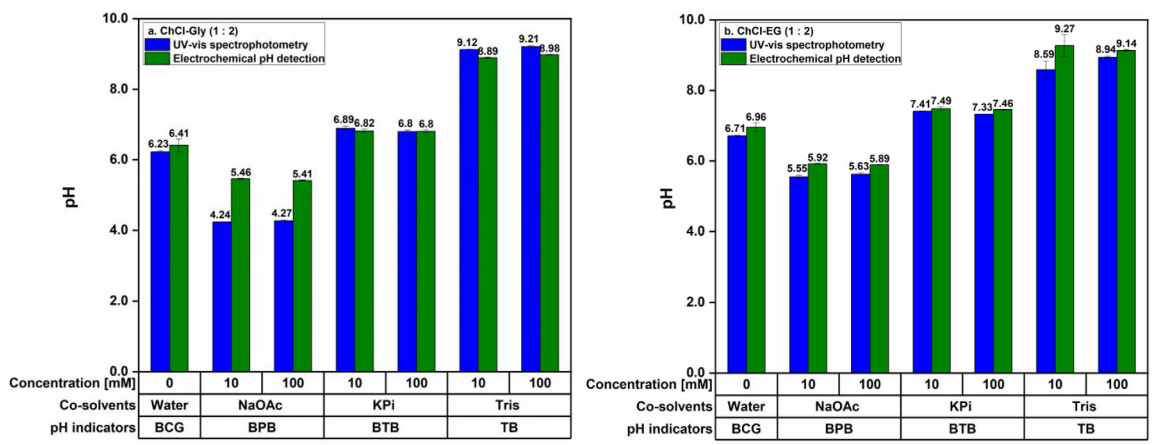

FIGURE 2 | Measured pH values for ChCl-Gly (1:2) (a) and ChCl-EG (1:2) (b) with 20 wt% water or buffer solutions, using a pH electrode (green bars) or UV–vis spectrophotometry with the addition of bromocresol green and bromophenol blue (absorbance at 591 and 615 nm, blue bars), NaOAC (pH 4.86) for ChCl-Gly and ChCl-EG, respectively, bromothymol blue (absorbance at 615 nm) KPi (pH 5.92) for ChCl-Gly and ChCl-EG, and tris buffer (pH 9.00) samples were measured using thymol blue (absorbance at 615 nm). All the experiments were conducted in triplicate. BCG: bromocresol green, BPB: bromophenol blue, BTB: bromothymol blue, and TB: thymol blue sodium salt.

pH values of Bet–Gly were reported to be 6.77 and 6.37, with water content of 30% and 50%, respectively. The increase in pH toward neutrality upon the addition of water (up to 80 wt%), on the other hand, can be caused by the gradual protonation of the eutectic medium until the establishment of an equilibrium. Both systems progressively reached the pH of pure water, indicating the transition from the DES-based medium to the DES-water medium, and finally to an aqueous solution.

Overall, the two pH measurement methods yielded comparable results. Just like for Case Study 1, we studied the effect of adding buffer (up to 20 wt% aqueous content), comparing the two pH analysis methods reported here. As noted in the experimental section (Supporting Information), three different buffers were evaluated to assess the effectiveness of pH, buffer type, and ionic strengths (10 and 100 mM) in controlling the final resulting DES formulations (Figure 4).

As in Case Study 1, the increase in buffer strength (from 10 to 100 mM) did not result in a significant pH shift. Here, the addition of KPi buffer, pH 5.92, did not result in a drastic pH change when compared to the addition of water, suggesting a possible dominant effect of the latter on the DES neutralization. On the other hand, more acidic and basic buffers, represented by NaOAc and tris, resulted in a more pronounced pH shift. As an example, NaOAc samples exhibited a pH of 6.01 and 6.43 for the electrochemical and photometric methods, in the case of Bet–Gly (1:2), and 6.11 and 6.60 for Bet-EG (1:3). Nevertheless, the proximity of the pH value of the added tris buffer to the DES medium resulted in a pH higher than 9.0 in all the analyzed samples. The highest measured

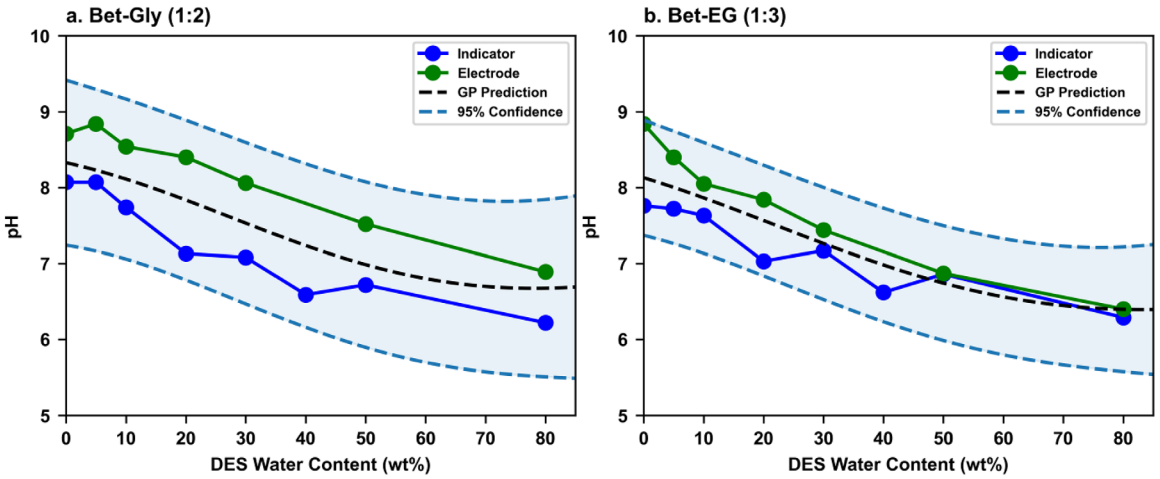

FIGURE 3 | Measured pH values for Bet-Gly (1:2) (a) and Bet-EG (1:3) (b) with different water fractions, using UV–vis spectrophotometry with the addition of bromothymol blue (absorbance at 615 nm, blue line), and using an electrochemical pH detector (green line). All measurements were conducted in triplicate. Predictions (black dashed line) with 95% confidence (blue dashed lines) intervals from GP models simultaneously fit to both data sources are also included.

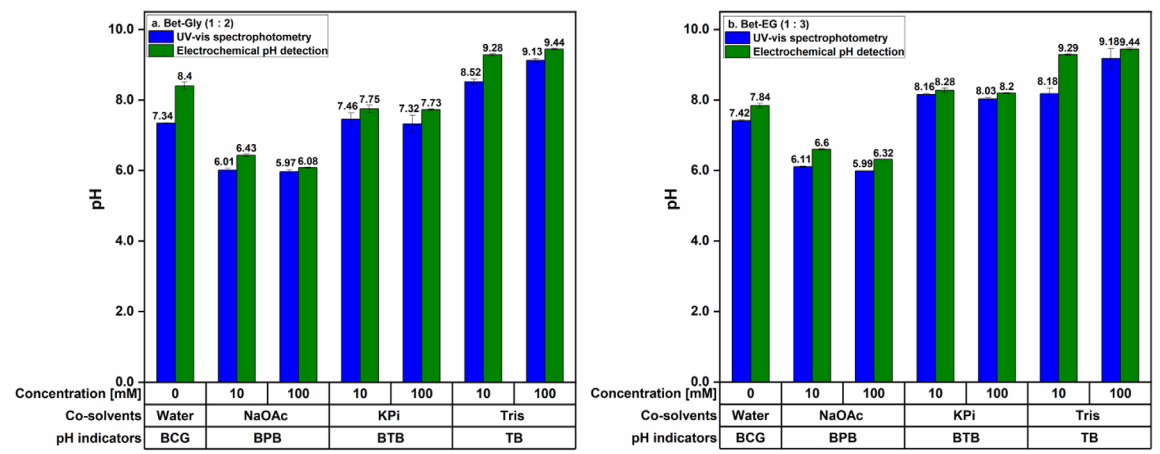

FIGURE 4 | Measured pH values for Bet-Gly (1:2) (a) and Bet-EG (1:3) (b) with 20 wt% water or aqueous buffer solutions, using a pH electrode (green bars) or UV–vis spectrophotometric measurements (blue bars). The NaOAc (pH 4.68) and KPi (pH 5.92) buffer samples were measured using bromophenol blue (591 nm) and bromothymol blue (615 nm), and tris buffer (pH 9.00) samples were measured using thymol blue (430 nm). All the experiments were conducted in triplicate. BCG: bromocresol green, BPB: bromophenol blue, BTB: bromothymol blue, and TB: thymol blue sodium salt.

value was 9.44 using the photometric method for both Gly and EG, using them as HBDs.

This additional set of experiments confirms the similar behavior of the two Bet-based systems, likely related to the same number of hydroxyl groups in both mixtures. Furthermore, it can be hypothesized that the buffer does not interfere with the two experimental methods used, as evidenced by the similar and comparable pH values.

2.4 | Case Study 3—Tetrabutylammonium Chloride–Based DES

Herein, the TBAC was used as an HBA, exhibiting the strongest acidic behavior among the three case studies introduced so far (Figure 5).

As shown in Figure 5a, the neat TBAC-Gly (1:3) exhibited an acidic pH (2.58 and 1.88 from the spectrophotometric and the electrochemical detection, respectively). Despite the different values, both fall within the GP-predicted 95% confidence interval, which, for that water content, is roughly 1 pH unit. Neat TBAC-EG (1:3) showed a pH of 3.44 and 4.43, as determined by the two methods (Figure 5b), with the indicator result (pH of 3.44) lying slightly outside the GP-predicted confidence interval. Quite contradictory was the comparison with literature [51] (Table 2), where values of 6.51–6.11 and 9.20–7.72 for TBAC-Gly (1:3) and TBAC-EG (1:3), respectively, across the temperature range of 293.15–353 K, were reported. Interestingly, the addition of 5 wt% of water leads to a significant pH increase, reaching 2.86 by electrochemical detection and 2.65 by the spectrophotometric method, for the glycerol one. Further addition of water results in a less pronounced neutralizing effect, with only a 1.1-unit pH increase between 5 and 80 wt% water content. The ethylene glycol

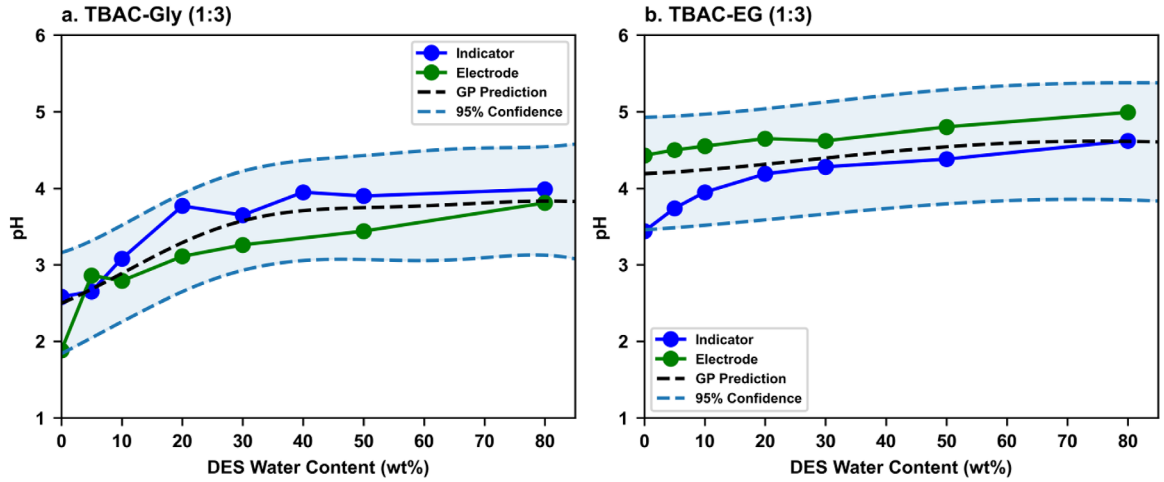

FIGURE 5 | Measured pH values for TBAC-Gly (1:3) (a) and TBAC-EG (1:3) (b) with different water fractions, using UV–vis spectrophotometry with the addition of bromothymol blue for (a) and bromocresol green for (b) (absorbance at 615 nm, blue line), and using an electrochemical pH detector (green line). All measurements were conducted in triplicate. Predictions (black dashed line) with 95% confidence (blue dashed lines) intervals from GP models simultaneously fit to both data sources are also included.

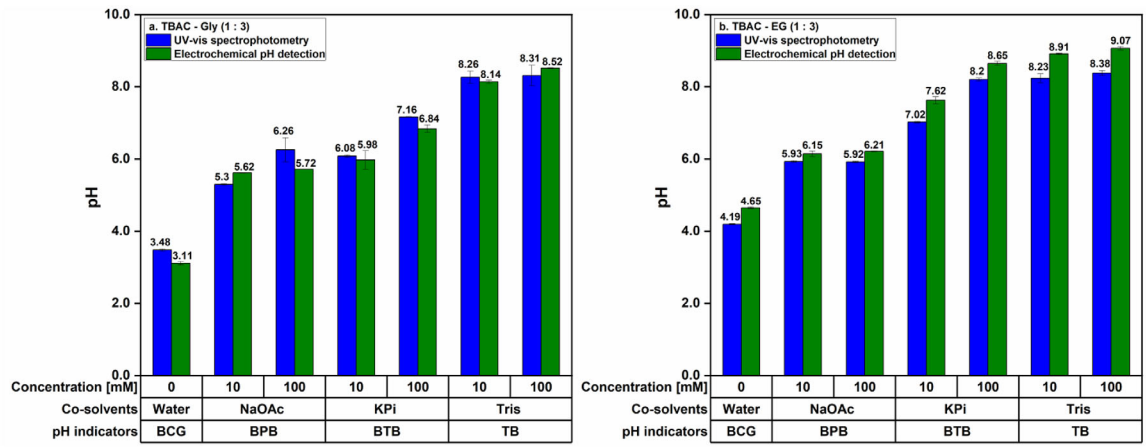

FIGURE 6 | The measured pH values for TBAC-Gly (1:3) (a) and TBAC-EG (1:3) (b) with 20 wt% water or aqueous buffer solutions using a pH electrode (green bars) or UV–vis spectrophotometric measurements (blue bars). Sodium acetate (NaOAc pH 4.68) was measured with bromophenol blue (absorbance at 591 nm) for TBAC-Gly and TBAC-EG. Potassium phosphate (KPi, pH 5.92) buffer was measured with bromothymol blue for both samples (absorbance at 615 nm), and tris buffer (pH 9.00) samples were measured using thymol blue (absorbance at 430 nm). All the experiments were conducted in triplicate. BCG: bromocresol green, BPB: bromophenol blue, BTB: bromothymol blue, and TB: thymol blue sodium salt.

mixture showed a similar behavior with an increasing pH until 4.99 and 4.62 with 80 wt% water. Interestingly, here, the addition of water resulted in an increase in pH rather than a decrease as had been observed in the ChCl- and Bet-based DESs. On the other hand, the addition of 20 wt% of buffer resulted in a more substantial shift toward the pH of the aqueous solution (Figure 6).

In the case of TBAC-based DESs, in contrast to the two case studies described above, the addition of different buffer strengths (10 and 100 mM) resulted in a more pronounced pH change across all the examined mixtures. For instance, increasing the KPi buffer concentration tenfold resulted in an increase of the pH by approximately 1 unit. Interestingly, both methods recorded the pH values higher than the inherent pH of the buffer systems studied (NaOAc, KPi). This behavior could be attributed to the propensity of TBAC to undergo ion exchange with the buffer components (salt metathesis) or to the formation of new ionic interactions with the phosphate or acetate groups, which are responsible for the acidic nature of the respective buffers.

2.5 | Case Study 4—Lidocaine-Based DES

The Lid-OA (1:1) DES was selected as a representative system for the class of hydrophobic DESs. Interestingly, the dynamic viscosity of the Lid-OA (1:1) DES increased with rising water content, a phenomenon known as the "thickening effect", eventually leading to the formation of a gel-like system. This behavior was evaluated by Zhang et al. [49], who assessed the phase behavior of DESs and DES-water mixtures containing 5–90 wt% water at a 0.5°C gradient. In particular, the Lid-based DESs exhibited thermo-switchable hydrophobicity with lower critical solution temperatures (LCST) ranging from 25°C to 33°C, the lowest value

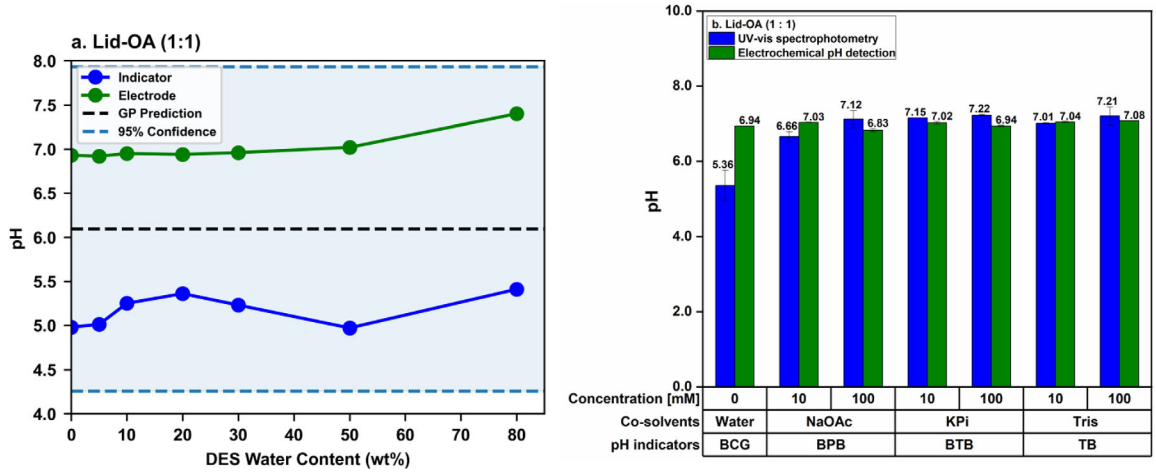

FIGURE 7 | Effect of increasing mass fraction of water on the pH of Lid-OA (1:1) (a). The green line represents the results from electrochemical detection, and the blue line represents the results from spectrophotometric detection with the addition of bromocresol green. All measurements were conducted in triplicate. Predictions (black dashed line) with 95% confidence (blue dashed lines) intervals from GP models simultaneously fit to both data sources are also included. Comparison of the pH values of Lid-OA (1:1) (b) measured with the electrochemical method (green bar) and UV–vis spectrophotometric method (blue bars) after the addition of 20 wt% water, 10 or 100 mM NaOAc (pH 4.68), KPi (pH 5.92), or tris buffer (pH 9.00) measured with bromocresol green (absorbance at 615 nm) bromophenol blue (absorbance at 591 nm), bromothymol blue (absorbance at 615 nm), and Thymol blue (absorbance at 430 nm), respectively. All measurements were conducted in triplicate.

(25°C) being observed at 30–50 wt% water. It seems that this switchable hydrophobicity is driven by water's effect on ionic equilibria. Longeras et al. [48] observed the DES de-mixing using infrared spectroscopy (IR) and attributed the phase separation between water and DES to the decrease of the ionic forms of Lid and OA, more soluble in water than the Lid and OA molecules. For this reason, measurements using both methodologies were not as straightforward as with the hydrophilic DESs (Case Studies 1–3). In the case of UV–vis spectrophotometric analysis, solubilizing the dye in the DES before measurement proved challenging, while the high viscosity of the system limited the performance of the electrode-based measurements. This resulted in a discrepancy between all the measured pH values using the two pH analysis methods (Figure 7), which GP modeling was unable to reconcile.

As shown in Figure 7a, no significant differences in the pH values were detected upon water addition. The pH detected using the spectrophotometer analysis (blue line) revealed a moderately acidic pH ranging from 4.80 (0 wt%) to 5.41 (80 wt%). On the other hand, pH electrode measurements (green line) displayed more neutral values ranging from 6.93 (0 wt% water) to 7.40 (80 wt% water). A pH value of 7.2 for the aqueous solution of DES 1:1 (50 wt%) was also reported by Longeras et al. (2020) [48]. Furthermore, no response was observed in the DES-buffer mixture regardless of the added buffer species (Figure 7b).

The peculiar properties and behavior of this DES could explain the lack of water and buffer tuning effects related to different proton activities. Nevertheless, further experiments are needed to elucidate the pH response in hydrophobic DESs, where the thickening effect of increasing the water content may lead to a different proton mass transfer, influencing the measurements with both methods.

3 | Conclusion

A synergistic approach has been conducted combining the experimental pH detection methods with stochastic ML modeling. The pH of the DESs was determined using two methods: (i) electrochemical sensing with a glass pH electrode, and (ii) molecular dye indicators, where protonation or deprotonation of pH-sensitive dyes was analyzed by UV–vis spectroscopy for a selected set of DES representatives. The two wet-lab methods, jointly fitted with a single GP model, were proven to be solid for hydrophilic DESs, with a discrepancy of up to 1 unit of pH maximum, where water can be blended and the dyes can be solubilized. Conversely, large discrepancies were observed when hydrophobic DES (Case 4 DES; Lid:OA) were used, and more research will be needed to understand the factors that govern the way of how pH can be measured in this type of DESs.

For ChCl- and Bet-based DESs (Case 1 and Case 2 DES), where the measured pH values ranged around neutrality and alkalinity, respectively, the addition of water led to a decrease in the pH. This behavior was found to be in line with the literature data. For TBAC-based DESs (Case 3 DES), which displayed an acidic pH, the increase in water content was correlated with a higher pH value. The buffer addition played a role in the pH modulation. Interestingly, relatively low buffer concentration, such as 10 mM, was found to be sufficient to withdraw some protons and equilibrate the DES-buffer to the buffer's pH in the ChCl- and Bet-based DESs. Remarkably, the result with TBAC-based DESs showed that even acidic DES can be basified with buffer contents, and that increasing the buffer strength, the shift is more pronounced. The addition of buffer, aimed to modulate the pH of DESs using a straightforward strategy, as in an aqueous system, then turns out to create a new DES-medium where the properties of the starting one might be changed (and interestingly, gradient-wise). However, further studies in this regard must

be carried out to see how the physical-chemical properties of these solvents are affected upon the addition of a buffer chosen specifically for every case.

Furthermore, the implementation of DESs in biocatalytic applications and bioprocesses urges continuous monitoring of the pH systems while the desired reaction takes place. This is especially important in cases where DESs are used as reaction media, with either water or buffers as co-solvents, given that the overall pH value of the reaction is the result of the contributions of each component in said system. Future experiments with continuous pH measurement would enlighten whether the acidity of the medium changes as substrates are converted into products (e.g., in esterification reactions). Therefore, we recommend measuring the pH before and after the substrate addition, as some substrates may trigger proton changes and alter the pH.

Several studies have reported pH values for well-established DES systems, providing useful benchmarks for comparing their acidity and guiding their selection for specific applications. Nevertheless, considerable uncertainty remains, not only as mentioned above, because the reported values often vary depending on factors such as the water content, the HBA-HBD molar ratio, and temperature, but also for the measurement defined by the protocol itself. As a result, the same DES can display noticeably different pH values across studies, and the nature of the HBD and HBA seems to have a substantial effect on the acidity of DESs.

The development of methods capable of continuously monitoring pH changes in real-time during reactions is essential. Such tools could allow direct observation of how the conversion of reactants to products (R → P) alters the proton environment, providing a deeper understanding of biocatalytic processes in DES-based systems.

As demonstrated in this paper, the use of pH indicators in DESs enables continuous monitoring of the chemical environment in specific biocatalytic applications, in particular for hydrophilic DESs. From all this, we can establish that pH indicator molecules can be employed to develop preliminary protocols for pH assessment in DES-based media, particularly when organic reactions are involved.

Acknowledgments

This project has received funding from the European Union's HorizonEurope research and innovation programme under the Marie Skłodowska-Curie grant agreement no. 101072731. The authors gratefully acknowledge the funding from the German Research Foundation (Deutsche Forschungsgemeinschaft, DFG) under the grant no. 528814716 (DFG FOR 5730, DESMOL2PRO). DOA and JAPC acknowledge the project CICECO-Aveiro Institute of Materials, UID/50011/2025 (DOI 10.54499/UID/50011/2025) & LA/P/0006/2020 (DOI 10.54499/LA/P/0006/2020) & UID/PRR/50011/2025 (DOI 10.54499/UID/PRR/50011/2025), financed by national funds through the FCT/MCTES (PIDDAC). The authors also acknowledge Dr. Leandro Silveri (New York University, Abu Dhabi) for his valuable contribution to refining the Python code used for data analysis. The text of this manuscript was reviewed and linguistically refined using ChatGPT (OpenAI, GPT-5). The scientific content, data interpretation, and conclusions are entirely the authors' own work.

Open access funding enabled and organized by Projekt DEAL.

Conflicts of Interest

The authors declare no conflicts of interest.

Data Availability Statement

The data that support the findings of this study are available from the corresponding author upon reasonable request.

References

1. T. Lemaoui, F. Abu Hatab, and A. S. Darwish, et al., "Molecular-Based Guide to Predict the pH of Eutectic Solvents: Promoting an Efficient Design Approach for New Green Solvents," *ACS Sustainable Chemistry & Engineering* 9 (2021): 5783–5808, https://doi.org/10.1021/acssuschemeng.0c07367.

2. A. Kyriakoudi, I. Radojčić Redovniković, and S. Vidović, et al., "Coupling Deep Eutectic Solvents With Innovative Extraction Techniques Towards Plant Derived Bioactive Compositions," *RSC Sustainability* 2 (2024): 1675–1691.

3. N. Zhang, P. Domínguez de María, and S. Kara, "Biocatalysis for the Synthesis of Active Pharmaceutical Ingredients in Deep Eutectic Solvents: State-of-the-Art and Prospects," *Catalysts* 14 (2024): 84.

4. E. L. Smith, A. P. Abbott, and K. S. Ryder, "Deep Eutectic Solvents (DESs) and Their Applications," *Chemical Reviews* 114 (2014): 11060–11082, https://doi.org/10.1021/cr300162p.

5. B. B. Hansen, S. Spittle, B. Chen, et al., "Deep Eutectic Solvents: A Review of Fundamentals and Applications," *Chemical Reviews* 121 (2021): 1232–1285.

6. D. O. Abranches and J. A. P. Coutinho, "Everything You Wanted to Know About Deep Eutectic Solvents but Were Afraid to Be Told," *Annual Review of Chemical and Biomolecular Engineering* 14 (2025): 2023.

7. H. Vanda, Y. Dai, E. G. Wilson, R. Verpoorte, and Y. H. Choi, "Green Solvents From Ionic Liquids and Deep Eutectic Solvents to Natural Deep Eutectic Solvents," *Comptes Rendus Chimie* 21 (2018): 628–638, https://doi.org/10.1016/j.crci.2018.04.002.

8. M. Panić, M. Radović, M. Cvjetko Bubalo, et al., "Prediction of pH Value of Aqueous Acidic and Basic Deep Eutectic Solvent Using COSMO-RS σ Profiles' Molecular Descriptors," *Molecules* 27 (2022): 4489.

9. F. Mohd Fuad and M. Mohd Nadzir, "The Formulation and Physicochemical Properties of Betaine-Based Natural Deep Eutectic Solvent," *Journal of Molecular Liquids* 360 (2022): 119392.

10. M. Rogošić, A. Damjanović, and M. Logarušić, "Solid-Liquid Phase Behaviour of Novel Kosmotrope/Chaotrope Binary Mixtures Involving Sarcosine," *Journal of Molecular Liquids* 413 (2024): 125944.

11. H. J. Hayler and S. Perkin, "The Eutectic Point in Choline Chloride and Ethylene Glycol Mixtures," *Chemical Communications* 58 (2022): 12728–12731, https://doi.org/10.1039/D2CC04008E.

12. M. Abate, G. Bontempelli, and N. Dossi, "Acid-Base Equilibria in Ethaline. An Approach Providing a Strategy for the pH Modulation in Deep Eutectic Solvents," *Journal of Molecular Liquids* 436 (2025): 128264.

13. R. A. Sheldon and J. M. Woodley, "Role of Biocatalysis in Sustainable Chemistry," *Chemical Reviews* 118 (2018): 801–838, https://doi.org/10.1021/acs.chemrev.7b00203.

14. J. T. Gorke, F. Srienc, and R. J. Kazlauskas, "Hydrolase-Catalyzed Biotransformations in Deep Eutectic Solvents," *Chemical Communications* 10 (2008): 1235–1237.

15. M. M. Nolasco, S. N. Pedro, C. Vilela, et al., "Water in Deep Eutectic Solvents: New Insights From Inelastic Neutron Scattering Spectroscopy," *Frontiers in Physics* 10 (2022): 834571.

16. A. S. D. Ferreira, R. Craveiro, A. R. Duarte, S. Barreiros, E. J. Cabrita, and A. Paiva, "Effect of Water on the Structure and Dynamics of Choline

Chloride/Glycerol Eutectic Systems," *Journal of Molecular Liquids* 342 (2021): 117463.

17. M. Tiecco, A. Grillo, E. Mosconi, W. Kaiser, T. Del Giacco, and R. Germani, "Advances in the Development of Novel Green Liquids: Thymol/Water, Thymol/Urea and Thymol/Phenylacetic Acid as Innovative Hydrophobic Natural Deep Eutectic Solvents," *Journal of Molecular Liquids* 364 (2022): 120043.

18. H. Kivelä, M. Salomäki, and P. Vainikka, "Effect of Water on a Hydrophobic Deep Eutectic Solvent," *Journal of Physical Chemistry B* 126 (2022): 513–527, https://doi.org/10.1021/acs.jpcb.1c08170.

19. O. Olawuyi, M. B. Bin Rafiq, and S. Ahmed, "Investigating the Impact of Water on a Menthol-Based Deep Eutectic Solvent: A Combined Experimental and Molecular Dynamics Study," *Industrial & Engineering Chemistry Research* 63 (2024): 20475–20485, https://doi.org/10.1021/acs.iecr.4c02346.

20. R. Craveiro, V. I. B. Castro, and M. T. Viciosa, "Influence of Natural Deep Eutectic Systems in Water Thermal Behavior and Their Applications in Cryopreservation," *Journal of Molecular Liquids* 329 (2021): 115533.

21. P. Kalhor, Y. Z. Zheng, H. Ashraf, B. Cao, and Z. W. Yu, "Influence of Hydration on the Structure and Interactions of Ethaline Deep-Eutectic Solvent: A Spectroscopic and Computational Study," *ChemPhysChem* 21 (2020): 995–1005, https://doi.org/10.1002/cphc.202000165.

22. Y. Dai, G. J. Witkamp, R. Verpoorte, and Y. H. Choi, "Tailoring Properties of Natural Deep Eutectic Solvents With Water to Facilitate Their Applications," *Food Chemistry* 187 (2015): 14–19, https://doi.org/10.1016/j.foodchem.2015.03.123.

23. C. Ma, A. Laaksonen, C. Liu, X. Lu, and X. Ji, "The Peculiar Effect of Water on Ionic Liquids and Deep Eutectic Solvents," *Chemical Society Reviews* 47 (2018): 8685–8720, https://doi.org/10.1039/C8CS00325D.

24. T. El Achkar and S. Fourmentin, "Deep Eutectic Solvents: An Overview on Their Interactions With Water and Biochemical Compounds," *Journal of Molecular Liquids* 288 (2019): 11028.

25. Q. Gao, Y. Zhu, X. Ji, W. Zhu, L. Lu, and X. Lu, "Effect of Water Concentration on the Microstructures of Choline Chloride/Urea (1:2)/Water Mixture," *Fluid Phase Equilibria* 470 (2018): 134–139, https://doi.org/10.1016/j.fluid.2018.01.031.

26. C. D'Agostino, L. F. Gladden, and M. D. Mantle, "Molecular and Ionic Diffusion in Aqueous—Deep Eutectic Solvent Mixtures: Probing Inter-Molecular Interactions Using PFG NMR," *Physical Chemistry Chemical Physics* 17 (2015): 15297–15304, https://doi.org/10.1039/C5CP01493J.

27. F. Gabriele, M. Chiarini, R. Germani, M. Tiecco, and N. Spreti, "Effect of Water Addition on Choline Chloride/Glycol Deep Eutectic Solvents: Characterization of Their Structural and Physicochemical Properties," *Journal of Molecular Liquids* 291 (2019): 111301.

28. I. Delso, C. Lafuente, J. Muñoz-Embid, and M. Artal, "NMR Study of Choline Chloride-Based Deep Eutectic Solvents," *Journal of Molecular Liquids* 290 (2019): 11236.

29. O. S. Hammond, D. T. Bowron, and K. J. Edler, "The Effect of Water Upon Deep Eutectic Solvent Nanostructure: An Unusual Transition From Ionic Mixture to Aqueous Solution," *Angewandte Chemie* 129 (2017): 9914–9917, https://doi.org/10.1002/ange.201702486.

30. G. Di Carmine, A. P. Abbott, and C. D'Agostino, "Deep Eutectic Solvents: Alternative Reaction Media for Organic Oxidation Reactions," *Reaction Chemistry & Engineering* 6 (2021): 582–598, https://doi.org/10.1039/D0RE00458H.

31. M. Cvjetko Bubalo, T. Andreou, M. Panić, M. Radović, and K. Radošević, "Natural Multi-Osmolyte Cocktails Form Deep Eutectic Systems of Unprecedented Complexity: Discovery, Affordances and Perspectives," *Green Chemistry* 25 (2023): 3398–3417, https://doi.org/10.1039/D2GC04796A.

32. V. Jančíková, M. Jablonský, K. Voleková, and I. Šurina, "Summarizing the Effect of Acidity and Water Content of Deep Eutectic Solvent-Like Mixtures—A Review," *Energies* 15 (2022): 9333.

33. V. Jančíková, V. Majová, and M. Jablonský, "Acidity and PH of DES-Like Mixtures and the Possibilities of Their Determination," *Journal of Molecular Liquids* 394 (2024): 123728.

34. A. P. Abbott, S. S. M. Alabdullah, A. Y. M. Al-Murshedi, and K. S. Ryder, "Brønsted Acidity in Deep Eutectic Solvents and Ionic Liquids," *Faraday Discussions* 206 (2018): 365–377, https://doi.org/10.1039/C7FD00153C.

35. Y. Zhu, T. X. Yang, B. K. Qi, H. Li, Q. S. Zhao, and B. Zhao, "Acidic and Alkaline Deep Eutectic Solvents (DESs) Pretreatment of Grapevine: Component Analysis, Characterization, Lignin Structural Analysis, and Antioxidant Properties," *International Journal of Biological Macromolecules* 236 (2023): 123977.

36. N. Rodriguez Rodriguez, L. MacHiels, and K. Binnemans, "P-Toluenesulfonic Acid-Based Deep-Eutectic Solvents for Solubilizing Metal Oxides," *ACS Sustainable Chemistry & Engineering* 7 (2019): 3940–3948, https://doi.org/10.1021/acssuschemeng.8b05072.

37. C. Li, D. Li, and S. Zou, "Extraction Desulfurization Process of Fuels With Ammonium-Based Deep Eutectic Solvents," *Green Chemistry* 15 (2013): 2793–2799, https://doi.org/10.1039/c3gc41067f.

38. J. Yin, J. Wang, and Z. Li, "Deep Desulfurization of Fuels Based on an Oxidation/Extraction Process With Acidic Deep Eutectic Solvents," *Green Chemistry* 17 (2015): 4552–4559.

39. C. Liu and J. Shi, "Understanding Lipase-Deep Eutectic Solvent Interactions Towards Biocatalytic Esterification," *Catalysts* 15 (2025): 358.

40. E. K. Baby, R. Savitha, G. K. Kinsella, B. J. Ryan, K. Nolan, and G. T. M. Henehan, "Structural and Mechanistic Insights Into Activators of Alcohol Dehydrogenase," *International Journal of Biological Macromolecules* 330 (2025): 148040, https://doi.org/10.1016/j.ijbiomac.2025.148040.

41. P. Xu, P. X. Du, M. H. Zong, N. Li, and W. Y. Lou, "Combination of Deep Eutectic Solvent and Ionic Liquid to Improve Biocatalytic Reduction of 2-Octanone With Acetobacter Pasteurianus GIM1.158 Cell," *Scientific Reports* 6 (2016): 26158.

42. J. P. Bittner, N. Zhang, L. Huang, P. Domínguez De María, S. Jakobtorweihen, and S. Kara, "Impact of Deep Eutectic Solvents (DESs) and Individual Des Components on Alcohol Dehydrogenase Catalysis: Connecting Experimental Data and Molecular Dynamics Simulations," *Green Chemistry* 24 (2022): 1120–1131, https://doi.org/10.1039/D1GC04059F.

43. A. Hayyan, F. S. Mjalli, and I. M. Alnashef, "Fruit Sugar-Based Deep Eutectic Solvents and Their Physical Properties," *Thermochimica Acta* 541 (2012): 70–75, https://doi.org/10.1016/j.tca.2012.04.030.

44. A. Hayyan, F. S. Mjalli, I. M. Alnashef, Y. M. Al-Wahaibi, T. Al-Wahaibi, and M. A. Hashim, "Glucose-Based Deep Eutectic Solvents: Physical Properties," *Journal of Molecular Liquids* 178 (2013): 137–141, https://doi.org/10.1016/j.molliq.2012.11.025.

45. A. Skulcova, A. Russ, M. Jablonsky, and J. Sima, "The pH Behavior of Seventeen Deep Eutectic Solvents," *BioResources* 13, no. 3 (2018): 5042–5051.

46. A. Mitar, M. Panić, and J. Prlić Kardum, "Physicochemical Properties, Cytotoxicity, and Antioxidative Activity of Natural Deep Eutectic Solvents Containing Organic Acid," *Chemical and Biochemical Engineering Quarterly* 33 (2019): 1–18.

47. F. Zhou, R. Shi, Y. Wang, Z. Xue, B. Zhang, and T. Mu, "Acidity Scales of Deep Eutectic Solvents Based on IR and NMR," *Physical Chemistry Chemical Physics* 24 (2022): 16973–16978, https://doi.org/10.1039/D2CP01816K.

48. O. Longeras, A. Gautier, K. Ballerat-Busserolles, and J. M. Andanson, "Deep Eutectic Solvent With Thermo-Switchable Hydrophobicity," *ACS Sustainable Chemistry & Engineering* 8 (2020): 12516–12520, https://doi.org/10.1021/acssuschemeng.0c03478.

49. N. Zhang, V. Lahmann, and J. P. Bittner, "Redox Biocatalysis in Lidocaine-Based Hydrophobic Deep Eutectic Solvents: Non-Conventional Media Outperform Aqueous Conditions," *ChemSusChem* 18 (2025): e202402075.

50. F. S. G. Bagh, K. Shahbaz, F. S. Mjalli, I. M. AlNashef, and M. A. Hashim, "Electrical Conductivity of Ammonium and Phosphonium Based Deep Eutectic Solvents: Measurements and Artificial Intelligence-Based Prediction," *Fluid Phase Equilibria* 356 (2013): 30–37, https://doi.org/10.1016/j.fluid.2013.07.012.

51. F. S. Mjalli, J. Naser, B. Jibril, V. Alizadeh, and Z. Gano, "Tetrabutylammonium Chloride Based Ionic Liquid Analogues and Their Physical Properties," *Journal of Chemical & Engineering Data* 59 (2014): 2242–2251, https://doi.org/10.1021/je5002126.

52. Y. T. Tan, G. C. Ngoh, and A. S. M. Chua, "Evaluation of Fractionation and Delignification Efficiencies of Deep Eutectic Solvents on Oil Palm Empty Fruit Bunch," *Industrial Crops and Products* 123 (2018): 271–277, https://doi.org/10.1016/j.indcrop.2018.06.091.

53. L. A. Rodrigues, M. Cardeira, and I. C. Leonardo, "Deep Eutectic Systems From Betaine and Polyols—Physicochemical and Toxicological Properties," *Journal of Molecular Liquids* 335 (2021): 116201.

54. H. Monteiro, A. Paiva, A. R. C. Duarte, and N. Galamba, "Structure and Dynamic Properties of a Glycerol–Betaine Deep Eutectic Solvent: When Does a DES Become an Aqueous Solution?," *ACS Sustainable Chemistry & Engineering* 10 (2022): 3501–3512, https://doi.org/10.1021/acssuschemeng.1c07461.

55. N. Bekavac, M. Radović, and A. Jurinjak, "Smart Design of Deep Eutectic Solvent-Based Aqueous Two-Phase Systems for Efficient Lipase Extraction," *Chemical Engineering Journal* 521 (2025): 166384.

56. E. Benítez-Correa, J. M. Bastías-Montes, S. Acuña-Nelson, and O. Muñoz-Fariña, "Effect of Choline Chloride-Based Deep Eutectic Solvents on Polyphenols Extraction From Cocoa (*Theobroma cacao* L.) Bean Shells and Antioxidant Activity of Extracts," *Current Research in Food Science* 7 (2023): 100614.

57. S. S. Alabdullah, "PH Measurements in Ionic Liquids," (Diss. University of Leicester, 2018).

58. S. Listiana, H. Bahua, and I. D. Utami, "Deep Eutectic Solvent as an Eco-Friendly Catalyst for the Synthesis of Hydroxyphenylglycine Methyl Ester," in *IOP Conference Series: Earth and Environmental Science* (2023), 1201.

59. A. A. Elgharbawy, A. Hayyan, and M. Hayyan, "Shedding Light on Lipase Stability in Natural Deep Eutectic Solvents," *Chemical and Biochemical Engineering Quarterly* 32 (2018): 359–370, https://doi.org/10.15255/CABEQ.2018.1335.

60. T. Sumiati, H. Suryadi, Harmita, and Sutriyo, "Comparison of the Deep Euteutic Solvent (DES) Solvent for Extracting Lignin From the Lignocellulosic Material of Pineapple Leaves," *Pharmacognosy Journal* 13 (2021): 1702–1709, https://doi.org/10.5530/pj.2021.13.219.

61. F. S. Mjalli and O. U. Ahmed, "Characteristics and Intermolecular Interaction of Eutectic Binary Mixtures: Reline and Glyceline," *Korean Journal of Chemical Engineering* 33 (2016): 337–343, https://doi.org/10.1007/s11814-015-0134-7.

62. P. Sombutsuwan, E. Durand, and K. Aryusuk, "Effect of Acidity/Alkalinity of Deep Eutectic Solvents on the Extraction Profiles of Phenolics and Biomolecules in Defatted Rice Bran Extract," *PeerJ Analytical Chemistry* 6 (2024): e29.

63. M. Logarušić, K. Šubar, and M. Nikolić, "Harnessing the Potential of Deep Eutectic Solvents in Biocatalysis: Design Strategies Using CO_2 to Formate Reduction as a Case Study," *Frontiers in Chemistry* 12 (2024): 1467810.

64. M. Panić, M. M. Elenkov, M. Roje, M. C. Bubalo, and I. R. Redovniković, "Plant-Mediated Stereoselective Biotransformations in Natural Deep Eutectic Solvents," *Process Biochemistry* 66 (2018): 133–139, https://doi.org/10.1016/j.procbio.2017.12.010.

65. Z. Teng, L. Wang, B. Huang, Y. Yu, J. Liu, and T. Li, "Synthesis of Green Deep Eutectic Solvents for Pretreatment Wheat Straw: Enhance the Solubility of Typical Lignocellulose," *Sustainability* 14 (2022): 657.

66. Z. Peng, Y. Wang, and W. Li, "Ultrasonic-Assisted Extraction of Flavonoids From *Amomum villosum* Lour. Using Natural Deep Eutectic Solvent: Process Optimization, Comparison, Identification, and Bioactivity," *Ultrasonics Sonochemistry* 116 (2025): 107304116.

67. R. Manurung, E. Naria, and A. G. Ilmi, and A. G. A. Siregar, "Utilizing a Deep Eutectic Solvent in Carotene Extraction Technology With Palm Methyl Ester Oil to Advance Green Technology," *Case Studies in Chemical and Environmental Engineering* 11 (2025): 101192.

68. M. Strobl, T. Rappitsch, S. M. Borisov, T. Mayr, and I. Klimant, "NIR-Emitting Aza-BODIPY Dyes—New Building Blocks for Broad-Range Optical pH Sensors," *Analyst* 141 (2016): 4028–4035.

69. C. E. Rasmussen, *Gaussian Processes in Machine Learning*, ed. O. Bousquet and G. Rätsch (Springer, 2004), 63–71.

70. J. P. Santos, F. H. B. Sosa, D. O. Abranches, and J. A. P. Coutinho, "Artificial Intelligence in the Discovery of Deep Eutectic Solvents With Lubricant Applications," *ACS Omega* 10 (2025): 43024–43033, https://doi.org/10.1021/acsomega.5c05944.

71. D. O. Abranches, W. Dean, M. Muñoz, et al., "Combining High-Throughput Experiments and Active Learning to Characterize Deep Eutectic Solvents," *ACS Sustainable Chemistry & Engineering* 12 (2024): 14218–14229, https://doi.org/10.1021/acssuschemeng.4c04507.

72. A. G. de G Matthews, M. van der Wilk, T. Nickson, et al., "GPflow: A Gaussian Process Library Using TensorFlow," *Journal of Machine Learning Research* 18 (2017): 1–6.

Supporting Information

Additional supporting information can be found online in the Supporting Information section.

The authors have cited additional references within the Supporting Information [68–72].

Supporting File: cctc70846-sup-0001-SuppMat.pdf.